

OPTIMIZING DIRECTIVITY PROPERTIES OF DSP CONTROLLED LOUDSPEAKER ARRAYS

G.W.J. van Beuningen Duran Audio BV, Zaltbommel, The Netherlands
E.W. Start Duran Audio BV, Zaltbommel, The Netherlands

ABSTRACT

This paper presents several issues related to the directivity aspects of loudspeaker arrays. Two optimization methods are described. A straightforward method that optimizes the main lobe of the far field polar pattern, and a more complex and versatile algorithm that is able to shape the directivity pattern in order to obtain a pre-defined direct SPL distribution over the listening area. Both methods will be illustrated with measured and simulated examples.

1 INTRODUCTION

The quality of a sound-reinforcement system benefits from the following conditions (with respect to a defined audience area):

- An evenly distributed Sound Pressure Level (SPL).
- Spectral uniformity.
- The direct SPL should be sufficiently higher than the diffuse SPL and the ambient noise level.

The first two conditions can generally be satisfied by any distributed sound system. The last condition, which is related to speech intelligibility [3], is more difficult to meet in spaces with 'complicated' acoustics (for example relatively small rooms with long reverberation times). The level of the diffuse (or reverberant) sound field can be minimized by 'projecting' the sound of the source(s) onto the relatively absorbing audience area while avoiding other surfaces. It is also helpful to limit the amount of sources that do not contribute to the direct sound.

In other words, there is a need to reduce the total amount of acoustical power and the level of discrete reflections (arriving after approx. 50 ms) without sacrificing the direct SPL. In this context, all sound arriving within approx. 20 ms after the first arrival is considered to contribute to the direct sound. If we restrict ourselves to electro-acoustical measures that can be taken to solve this problem, a source that is positioned a small offset above the audience area would be favorable. This source should have a very narrow opening angle in the direction perpendicular to the audience area (i.e. vertical for a horizontal audience plane) and a wide coverage in the audience plane itself (Fig 1).

The above described directivity criterion is practically impossible to realize for a wide frequency range with a horn or waveguide solution. In the next section we shall see that there is a good match between the natural directivity of a line source and this desired directivity.

2 GENERAL ARRAY DIRECTIVITY ISSUES

2.1 Frequency Dependency

A line source, continuous as well as a discrete version consisting of an arrayed collection of transducers (loudspeakers), exhibits a strong frequency dependence of the radiation pattern. The beam width collapses as the frequency increases. It can be shown [1,2] that at 'large' distances (i.e. in the far field) Eq (2-1) holds for the vertical directivity of the discrete line source represented in Fig 2. In this case N omni-directional sources are separated by a distance d , λ represents the wavelength.

$$G(\lambda, \theta) = \frac{\sin\left(\frac{N \cdot \pi \cdot d}{\lambda} \cdot \sin \theta\right)}{N \cdot \sin\left(\frac{\pi \cdot d}{\lambda} \cdot \sin \theta\right)} \quad \text{Eq (2-1)}$$

This equation can be approximated by:

$$G(\lambda, \theta) \approx \frac{\sin\left(\frac{\pi \cdot L}{\lambda} \cdot \sin \theta\right)}{\frac{\pi \cdot L}{\lambda} \cdot \sin \theta} \quad \text{Eq (2-2)}$$

$$\text{if } \left| \frac{\pi \cdot d}{\lambda} \cdot \sin \theta \right| \ll 1 \text{ and } L = N \cdot d$$

Eq (2-2) is the far field directivity function for a continuous line source with length L .

The occurrence of the $\sin(x)/x$ behavior in the previous equation is not surprising because it can be shown that the directivity function can be obtained by a spatial Fourier transform of the function that describes the source distribution (see for example [4,5]).

From Eq (2-2) can be derived that the -6 dB beam width ('opening angle') of the main lobe is:

$$BW_{-6dB} \approx 2 \cdot \sin^{-1}\left(\frac{1.9 \cdot \lambda}{L \cdot \pi}\right) \quad \text{Eq (2-3)}$$

For highly directive main lobes this can be approximated by:

$$BW_{-6dB} \approx 1.2 \cdot \frac{\lambda}{L} \text{ (in radians)} \quad \text{Eq (2-4)}$$

From Eq (2-4) it is clear that the beam width is inversely proportional to the array length L and linearly depending on the wavelength.

2.2 Beam Steering

By applying different delays to each transducer the main lobe can be 'steered' into a specific direction θ_0 . The far field directivity function of the equidistantly spaced, discrete array (Eq (2-1)) can be rewritten if the ℓ^{th} transducer in the array is delayed with a value $(\ell - 1) \cdot \tau$:

$$G(\lambda, \theta, \theta_0) = \frac{\sin\left(\frac{N \cdot \pi \cdot d}{\lambda} \cdot [\sin \theta - \sin \theta_0]\right)}{N \cdot \sin\left(\frac{\pi \cdot d}{\lambda} \cdot [\sin \theta - \sin \theta_0]\right)} \quad \text{Eq (2-5)}$$

$$\text{with } \sin \theta_0 = \frac{c \cdot \tau}{d} \quad \text{Eq (2-6)}$$

Eq (2-4) still holds for narrow main lobes and small values of the steering angle θ_0 . However there is a tendency for increased level of the side lobes and larger width of the main lobe as the absolute value of the steering angle increases. An example is shown in Fig 3, the directivity function of Eq (2-5) is plotted in dB as a function of θ for various values of θ_0 . For better comparison the non-zero θ_0 graphs are also centered around 0 deg.

2.3 Source Distribution

2.3.1 Spatial Aliasing

Careful examination of Eq (2-1) reveals that, besides the main lobe, maxima occur if:

$$|\sin \theta| = n \cdot \frac{\lambda}{d} \quad \text{with } n \text{ an integer } \geq 1 \quad \text{Eq (2-7)}$$

This can of course only occur if $d \geq \lambda$ holds (for real values of θ). Eq (2-7) can be rewritten as:

$$|\Delta r_\ell| = n \cdot \lambda \quad \text{Eq (2-8)}$$

which says that the maxima occur if the path length differences Δr_ℓ , from the individual array elements to the summation point in the far field, equal an integer number of wavelengths.

The maxima, so-called 'grating' lobes which are repetitions of the main lobe, originate from the fact that the array is too coarsely sampled (i.e. distance between the elements is too large compared to the wavelength).

In other words we can say that, analogous to the time - frequency discrete Fourier transform, the Shannon theorem must be obeyed to prevent 'spatial' aliasing. Spatial aliasing cannot occur if the distance between the array elements satisfies [4]:

$$\Delta z_\ell < \frac{1}{2} \cdot \lambda_{\min} \quad \text{Eq (2-9)}$$

which holds for the general case with $\Delta z_\ell = z_\ell - z_{\ell-1}$ and λ_{\min} belonging to the highest frequency that has to be reproduced by transducer ℓ .

Proceedings of the Institute of Acoustics

An example is given in Fig 4. The directivity function of an array, consisting of 16 omni-directional sources spaced at $d = 0.1$ m, is represented as a polar plot for two frequencies. It can be clearly seen that as the frequency goes up, the first maxima occur for $\theta = \pm 90^\circ$. In this so-called 'end-fire' region Eq (2-7) can be satisfied for the highest value of λ (lowest frequency). As the frequency increases even further, the grating lobes bend towards the main lobe and new ones emerge in the end-fire region as soon as Eq (2-7) is satisfied for the next value of n .

Note that in the level of the grating lobes may be reduced by:

- Using directional transducers.
- Non-equidistant spacing of the array elements.

2.3.2 Symmetrical versus a-Symmetrical Positioning

If the array elements are non-uniformly distributed over the line, we can distinct between symmetrical and a-symmetrical positioning schemes. Compared to an a-symmetrical scheme, symmetrical positioning generally lowers the level of the side lobes of the far field directivity function (at the expense of a somewhat wider main lobe). Note that this reduction can also be found for a uniformly sampled array if position dependent weighing of the contributions of the individual elements is applied. This 'windowing' or 'tapering' can be interpreted as a second analogy with the time - frequency Fourier transform.

Practical applications usually require that the array is mounted at a height slightly above the audience area in order to prevent blocking of the direct sound contributions of (some of) the transducers. In this case the a-symmetrical positioning scheme is favorable because, even without any processing (i.e. filtering), the near field SPL versus distance is already more constant and less dependent on the height of the listening area.

An illustration is shown in Fig 5 and Fig 6, 16 omni-directional sources are positioned according to an a-symmetrical and symmetrical logarithmic format. The lowest element is located at $z = 0$ m, the distance between the outermost elements is 1.5 m for both cases and the smallest element inter-distance is 0.05 m. Because Eq (2-1) does not hold in this general case we have to calculate the directivity function by a complex summation over all the array elements, so in this case the directivity is also correctly represented under near field conditions (see also Eq (3-5)).

The 1 kHz far field directivity (dashed curves) is compared against the directivity for the equidistant array (straight line, which is the same as in Fig 3). The 1 kHz SPL versus distance (log scale) plots are shown for three different receiver heights: $z = -0.5$ m (upper curves), -1.0 m and -1.5 m. The SPL at 100 m is set to an arbitrary level of 0 dB.

Proceedings of the Institute of Acoustics

2.4 Distance Dependency

For any real-life acoustical source it is important to discriminate between near field and far field conditions. In the far field of the source the wave propagation is purely spherical. Consequently the sound pressure level is inversely proportional to the measuring distance (the 'inverse square law' holds). The directivity is independent of the distance from the source to the measuring point. In the more complicated near field however, the directivity may heavily depend on the distance. In this section we will show that for long loudspeaker arrays, fairly large measuring distances are required to obtain true far field conditions. A large part of the audience area usually will be located in the near field, or in the near- to far field transition area, of the loudspeaker array.

Consider the representation of a line array as schematically shown in Fig 7. To be able to describe the directivity in the near field we need a reference point for the source. If the source was a simple enclosure with only one loudspeaker this reference point usually coincides with the acoustical center of the loudspeaker. In the case of a loudspeaker array however, no single acoustical center can be defined.

In the case of Fig 7, r represents the horizontal distance from the reference point to the measuring point P . L is the vertical distance from the reference point to the top of the array. For an asymmetrically configured array this distance is almost equal to the physical length of the radiating (i.e. active) part of the array. If the array configuration is symmetrical, the reference point will be in the center of the array. In the latter case L equals half of the length of the active part of the array.

One way of determining the beginning of the far field is to put a constraint on the coherency of the sound pressure contributions of the individual elements that make up the array. If we require that the maximum difference in path lengths from the individual transducers to point P is (much) smaller than half a wavelength the following equation will be the result [2]:

$$\sqrt{L^2 + r^2} - r < \frac{1}{2} \cdot \lambda \quad \text{Eq (2-10)}$$

In a first order approximation of the square root it can be shown that the following two conditions must hold:

$$\begin{aligned} r &\gg L \\ r &\gg \frac{L^2}{\lambda} \end{aligned} \quad \text{Eq (2-11)}$$

Especially the second condition will require large values for r in the case of long arrays if the frequency is high (small wavelengths).

3 OPTIMIZATION METHODS

3.1 Straightforward - Far Field Beam Forming

3.1.1 Description

The goal of this optimization method can be re-formulated as 'Shaping the main lobe while reducing the level of all other lobes', Fig 8.

To obtain a frequency independent shape of the main lobe, the effective array length should be made inversely proportional to the frequency (as was shown in Eq (2-4)):

$$L_{eff}(\lambda) = const \cdot \lambda \quad \text{with } const = \frac{69^\circ}{BW_{-6dB, Required}} \quad \text{Eq (3-1)}$$

Traditionally this was done by using some sort of acoustical filtering or by constructing nested sub-arrays. Here we will electronically filter the signals applied to the individual array elements.

The filters also have to:

- Compensate for the non-uniform density distribution of the sources.
- Correct for the varying number of active sources as a function of frequency.
- Introduce a position dependent weighing ('window') to reduce the level of the side lobes.

Refer to [4] for a detailed description.

Combining the spatial aliasing constraint described in Eq (2-9) with the frequency independent main lobe requirement of Eq (3-1) results in an optimum logarithmic positioning scheme of the transducers. Applying this scheme, described in [6], reduces the total number of transducers that is required for a given frequency range.

Beam steering can be introduced to aim the main lobe without the need for physical rotation of the array. For the individual channel delays the following equation must hold for the general (i.e. non-far field) case of a focused delay design:

$$\tau_t = \frac{D_F - r_t}{c} - \tau_t^{filter} + \tau_{offset} \quad \text{Eq (3-2)}$$

$$\text{with } r_t = \sqrt{D_F^2 - 2 \cdot D_F \cdot \sin \theta_0 \cdot (z_t - z_1) + (z_t - z_1)^2} \quad \text{Eq (3-3)}$$

In this case D_F represents the distance from the reference point (in this case z_1) to the focus point P (Fig 9). The distance of each element at z_t to P is given by r_t . θ_0 is the aiming angle (negative values point downwards) and τ_t^{filter} represents the filter group delay in the transition band. The correction τ_{offset} is required to make all delays positive.

3.1.2 Implementation

For maximum flexibility and control, Eq (3-1) to Eq (3-3) can be implemented within a Digital Signal Processor (DSP), see Fig 10. Because it is important that the output channel filters exhibit a linear phase (or constant group delay) in the transition band, they may be implemented as Bessel IIR (Infinite Impulse Response) filters. This reduces overall execution time compared to a FIR (Finite Impulse Response) solution. The IIR implementation requires an interpolation filter to improve (double) the time resolution for the channel delay buffer.

Proceedings of the Institute of Acoustics

The scheme shown in Fig 10 is implemented on a TMS320C32/50 floating point processor and calculates eight 4th order IIR filters in real-time together with the auxiliary processing for a sample frequency of 48 kHz.

As an example we will look at an a-symmetrically configured DSP controlled array, primarily designed for speech reinforcement [8]. This array contains 32 loudspeakers (of 4" diameter), driven in pairs by 16 individual channels. For high frequencies the application of Eq (3-1) is limited by the transducer size. For low frequencies the physical array length (which in this case is approx. 4.2 m) is the limiting factor.

Fig 11 shows the 'on axis' 1 kHz octave averaged SPL as a function of distance. The theoretical response for a line array in the near field (-3 dB per distance doubling) is also shown. The maximum value of L_{eff} is about 12λ for a frequency of 1 kHz. In order to meet the second condition of Eq (2-11), the measuring distance should be larger than 49 m. Note that excessive far field distances are avoided for higher frequencies, due to the reduction in effective length.

Fig 12 shows a comparison between the directivity in the case of a 'processed' and 'directly driven' (i.e. no processing) situation of the array. Refer to Fig 13 for an overview of simulated polar plots for various distances. Due to the location of the reference point, the beam apparently shifts upwards if the distance decreases. Note that even between the results at 30 m and 70 m there is a noticeable difference. SPL versus distance plots for the mid-band frequencies can be found in Fig 15.

Some drawbacks of the straightforward beam forming method are described in the following section.

3.1.3 Drawbacks

Complex Shapes of the Audience Area

The main lobe is difficult to optimize for complex shapes of the audience area. A traditional 'main floor with rear balcony' situation can be served by a single array generating two main lobes (see Fig 14 for an example). However the extra set of output filters and delays, that is required for an independently controllable second lobe, puts a severe claim on the DSP in terms of extra execution cycles. Furthermore interference patterns are likely to occur in the transition area between the two lobes. The situation gets even more complicated for curved or 'triple-deck' audience area shapes.

Optimizing the Performance

The performance of a loudspeaker array in a typical space is generally defined by the main lobe parameters ('opening angle', 'aiming angle' and 'focus distance') and the mounting height with respect to the average listening height. As a starting point the parameters related to the focus point can be geometrically optimized as indicated in Fig 15. The required 'opening angle' cannot be calculated from the geometrical model because the specified value is only valid in the far field. And, as already indicated, the near field may form the major part of the audience area for long arrays. Acoustical prediction software may help to optimize the performance of the array in the room [7,9], the best solution still has to be found while simulating on a 'trial-and-error' basis.

Listener Height

For parts of the audience area located close to the array, the SPL strongly depends on the listener height. This may be a problem if the audience contains standing as well as seated people.

A better control over the exact shape of the radiation pattern in the near field as well as the far field is required to overcome these disadvantages. This is described in the next section.

3.2 Complex - Radiation Pattern Shaping

3.2.1 Description

Consider the loudspeaker array configuration as shown in the y-z plane in Fig 16. The array consists of N loudspeakers (transducers), the position of the ℓ^{th} transducer is specified by r_{ℓ}^{tr} . A set of M receiver positions is defined on an arbitrary shaped line in the y-z plane. The position of receiver m is indicated with r_m^{rec} . The vertical (elevation) angle between transducer ℓ and receiver m is indicated by $\theta_{m,\ell}$ ($-90^\circ < \theta_{m,\ell} < 90^\circ$).

The distance between transducer ℓ and receiver m is specified by:

$$r_{m,\ell} = |r_m^{\text{rec}} - r_{\ell}^{\text{tr}}| \quad \text{Eq (3-4)}$$

The total response $P(r_m^{\text{rec}}, f)$ of the array at receiver position r_m^{rec} can be calculated by a complex summation of the contributions of the individual elements:

$$P(r_m^{\text{rec}}, f) = \sum_{\ell=1}^N W_{\ell}(f) \cdot G_{\ell}^b(\theta_{m,\ell}, f) \cdot \frac{e^{-j \cdot k \cdot r_{m,\ell}}}{r_{m,\ell}} \quad \text{Eq (3-5)}$$

with k representing the wavenumber, $k = \frac{\omega}{c}$ and c is the speed of sound.

In Eq (3-5), $W_{\ell}(f)$ represents the complex and frequency dependent weighing factor of the ℓ^{th} transducer. The far field vertical directivity of a single transducer is indicated by $G_{\ell}^b(\theta_{m,\ell}, f)$. This frequency dependent term may be different for each transducer and also includes its on-axis frequency response. Note that Eq (3-5) is also valid for receivers located in the near field of the array. The only restriction is that far field conditions for the individual loudspeakers must be satisfied for each receiver position. Eq (3-5) can be rewritten in matrix notation:

$$\vec{P} = \mathbf{H} \cdot \vec{W} \quad \text{Eq (3-6)}$$

$$\vec{P} = \begin{pmatrix} P(r_1^{\text{rec}}, f) \\ \vdots \\ P(r_m^{\text{rec}}, f) \\ \vdots \\ P(r_M^{\text{rec}}, f) \end{pmatrix} \quad \mathbf{H} = \begin{pmatrix} H_{1,1} & H_{1,2} & \dots & \dots & H_{1,N} \\ H_{2,1} & H_{2,2} & \vdots & & \vdots \\ \vdots & \vdots & \vdots & & \vdots \\ \vdots & \dots & H_{m,\ell} & \dots & \vdots \\ \vdots & \vdots & \vdots & & \vdots \\ \vdots & \vdots & \vdots & & \vdots \\ H_{M,1} & \dots & \dots & \dots & H_{M,N} \end{pmatrix} \quad \vec{W} = \begin{pmatrix} W_1(f) \\ \vdots \\ W_{\ell}(f) \\ \vdots \\ W_N(f) \end{pmatrix} \quad \text{Eq (3-7)}$$

$$\text{and } H_{m,\ell} = G_{\ell}^b(\theta_{m,\ell}, f) \cdot \frac{e^{-j \cdot k \cdot r_{m,\ell}}}{r_{m,\ell}} \quad \text{Eq (3-8)}$$

Proceedings of the Institute of Acoustics

Let \vec{D} represent a vector containing the desired target response for a specific frequency of the array on each receiver position p_m^{rec} :

$$\vec{D} = \begin{pmatrix} D(p_1^{rec}, f) \\ \vdots \\ D(p_m^{rec}, f) \\ \vdots \\ D(p_M^{rec}, f) \end{pmatrix} \quad \text{Eq (3-9)}$$

By replacing \vec{P} by the desired response \vec{D} Eq (3-6) can be re-written as the following system of equations with unknown weighing factors \vec{W} :

$$\mathbf{H} \cdot \vec{W} = \vec{D} \quad \text{Eq (3-10)}$$

There is no unique solution because in general there are more equations than variables ($M > N$). A best fit for \vec{W} can be found by applying the 'least-squares' algorithm to Eq (3-10):

$$\min_{\vec{W}} \left\{ \varepsilon = \left| \mathbf{H} \cdot \vec{W} - \vec{D} \right|^2 \right\} \quad \text{where the error } \varepsilon \text{ has to be minimized} \quad \text{Eq (3-11)}$$

Eq (3-11) can be extended with error weighing coefficients that depend on the receiver position p_m^{rec} . Compensation for a non-uniform distribution of the receiver positions can be realized in this way. It is then also possible to deliberately introduce differences in importance between the various receiver positions.

The total array response with optimum weighing factors has to be insensitive to small deviations in the positions and/or the directivity of the individual loudspeakers. Furthermore it is required that the optimum directivity solution does not suffer from a poor overall efficiency. A further extension of Eq (3-11) has been made to overcome these problems in order to obtain practical applicable optimum values for the weighing factors. This extension is beyond the scope of this paper and will not be discussed here.

By applying this modified variant of Eq (3-11), a complex filter response $W_\ell^{opt}(f)$ can be calculated for each transducer ℓ (for any required frequency). By inverse Fourier transforming $W_\ell^{opt}(f)$, the impulse response $w_\ell^{opt}(t)$ of filter ℓ will be obtained:

$$w_\ell^{opt}(t) = F^{-1} \{ W_\ell^{opt}(f) \} \quad \ell = 1, 2, \dots, N \quad \text{Eq (3-12)}$$

Note that the impulse responses are of infinite length in general. Finite length impulse responses (required for implementation of the filters in a DSP) can be obtained by windowing $w_\ell^{opt}(t)$. The filters should be made causal by shifting the windowed impulse responses with a time-delay that must be the same for each ℓ . The resulting coefficients can be implemented as FIR filters in a DSP.

3.2.2 Radiation Pattern Shaping Method - Example

To test the method described in the previous section, an array configuration according to Fig 17 was optimized. The symmetrical array consists of 16 individually controlled 4" loudspeakers indicated by the small triangles. The inter-distance of the center loudspeakers is 0.105 m, the distance between the centers of the two outer loudspeakers is 3.2 m. The transducer distribution over the array is non-uniform as indicated in Fig 17. The center of the array is located at an (arbitrary) height $z = 0$ m and the audience area is located at $z = -2.62$ m.

In this example we will try to optimize for a flat response on the audience area from $y = 5$ m to 50 m (indicated by the + symbols). The target level on the other receiver positions (indicated by the o symbols) should be as low as possible.

For the desired response \vec{D} of Eq (3-9) can be written:

$$\begin{cases} D(\vec{p}_m^{rec}, f) = 0 & \text{for } 0 \leq y_m^{rec} < 5, \quad z_m^{rec} = 0 \\ D(\vec{p}_m^{rec}, f) = e^{-jkr_m} & \text{for } 5 \leq y_m^{rec} \leq 50, \quad z_m^{rec} = 0 \\ D(\vec{p}_m^{rec}, f) = 0 & \text{for } y_m^{rec} = 50, \quad -3 \leq z_m^{rec} \leq 10 \\ D(\vec{p}_m^{rec}, f) = 0 & \text{for } 0 \leq y_m^{rec} < 50, \quad z_m^{rec} = 10 \end{cases} \quad \text{Eq (3-13)}$$

Note the occurrence of the delay term in the desired response on the audience area (this compensates for the differences in distance from the array to the receiver positions).

Fig 18 shows the shape of the simulated far field 3-D directivity for the optimized array at a frequency of 1 kHz.

Optimized SPL versus distance plots for the 8 octave bands (63 Hz to 8 kHz) can be found in Fig 19. The dotted lines show the simulation results (scaled to 0 dB) for the optimized ideal filters. The straight lines represent the simulated results for the windowed 64-pt FIR filters that were used in the test setup. From these graphs it is clear that the array is very well optimized to meet the target criterion (except for the lowest two frequency bands, due to the relatively limited array length). The 16 filters were implemented on two TMS320C32/50 floating point DSPs sampling at 24 kHz. The target SPL response as well as measured data is also indicated in the figures.

The results were verified against measurements (indicated by the dots in Fig 19). The array was mounted outside on a scaffold with the center of the array located at 4.32 m above the ground plane (grass). The measurement microphone was placed 1.7 m above the ground plane. The measurements show a good correlation with the simulations for the audience area, especially in the mid frequency bands. Due to the test setup, the lower frequency bands exhibit too much modulation by the inevitable ground reflection, so they are not shown here.

Simulated and measured far field vertical polar responses are shown in Fig 20. The measurements were taken at a distance of 32 m from the center (reference point) of the array. It is clear that the target response, here indicated by the 'pie-shaped' segments that are the same for all frequency bands, is very well approximated by the main lobe of the simulated response. The limited array length causes deviations in the lower frequency bands. The results in the 63 and 125 Hz bands also show that the directivity may be improved by increasing the FIR filter length. Another interesting feature is the increase in the level of the upwards aimed side- and grating lobes (i.e. into the direction opposite to the aiming of the main lobe) relative to the downwards aimed lobes. This can be very well observed for the frequency bands of 1 kHz and higher. The measurements follow the predictions very well.

4 CONCLUSION

Two methods of DSP assisted array optimization have been described:

Far field beam forming.

This method optimizes the shape of the far field main lobe. The method is straightforward, relatively easy to implement and requires modest computational power. It has however limitations that may restrict its application under specific circumstances.

Radiation pattern shaping.

A solution has been presented for the general problem of finding optimum channel filter coefficients given a loudspeaker array and an audience area configuration.

This method:

- Optimizes to a pre-defined direct SPL (and spectral) distribution over a specific audience area.
- Optimizes the directivity of the array in the near field as well as the far field (the wave field is optimized).
- Deals with complex shaped audience areas.
- Handles non-uniformly distributed arrays, non-linear arrays and/or arrays containing different types of transducers in a transparent way.
- Accounts for spectral corrections of the transducers ('equalizing') and 'cross-overs' if required.

The main disadvantage of the method is that due to its complexity a relatively long calculation time is required. Both off-line (during the calculation of the filter coefficients) as well as on-line (FIR implementation inside the DSP) calculation times are significantly higher compared to the first method.

Proceedings of the Institute of Acoustics

5 REFERENCES

1. H.F. Olson.
Acoustical Engineering, p 35 - 43 (1957).
2. L.E. Kinsler, A.R. Frey, A.B. Coppens & J.V. Sanders.
Fundamentals of Acoustics, Third edition, p 187 - 197 (1982).
3. T. Houtgast, H.J.M. Steeneken and R. Plomp.
Predicting Speech Intelligibility in Rooms from the Modulation Transfer Function.
Part I General Room Acoustics.
Acustica vol. 46, p 60 - 72 (1980).
4. M. van der Wal, E.W. Start and D. de Vries.
Design of Logarithmically Spaced Constant-Directivity Transducer Arrays.
J. Audio Eng. Soc. vol. 44 no. 6 , p 497 - 507 (1996).
5. D.L. Smith.
Discrete-Element Line Arrays - Their Modeling and Optimization.
J. Audio Eng. Soc. vol. 45 no. 11, p 949 - 964 (1997).
6. G. de Vries.
Loudspeaker System with Controlled Directional Sensitivity.
Patent EP 0 791 279 B1 (1995).
7. B.I. Dalenbäck.
Verification of prediction based on randomized tail-corrected cone-tracing and array modeling.
Presented at the ASA/EAA Berlin conference (1999).
8. Intellivox-6c datasheet.
www.duran-audio.com.
9. CATT Acoustic.
www.netg.se/~catt.

FIGURES

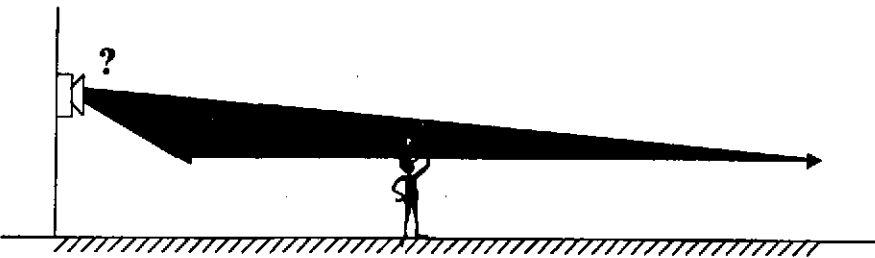


Fig 1 Cross section of 'ideal' directivity pattern.

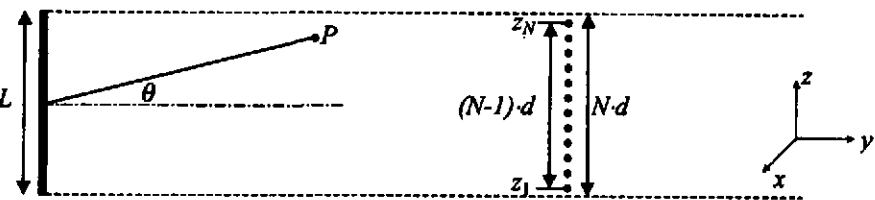


Fig 2 Continuous and discrete version of a line source with length L .

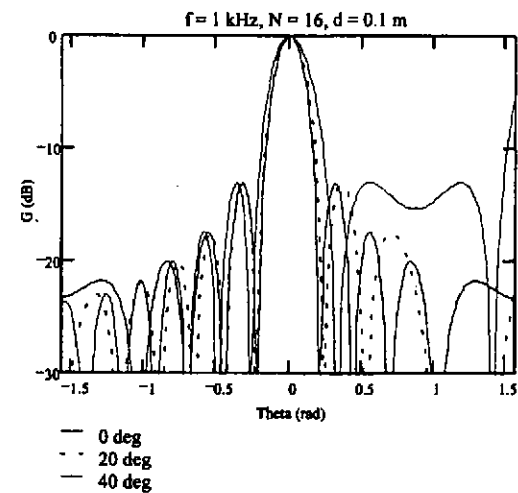


Fig 3 Directivity as a function of θ ($-90^\circ < \theta < 90^\circ$) for θ_0 is 0° , 20° and 40° , shifted to $\theta = 0^\circ$.

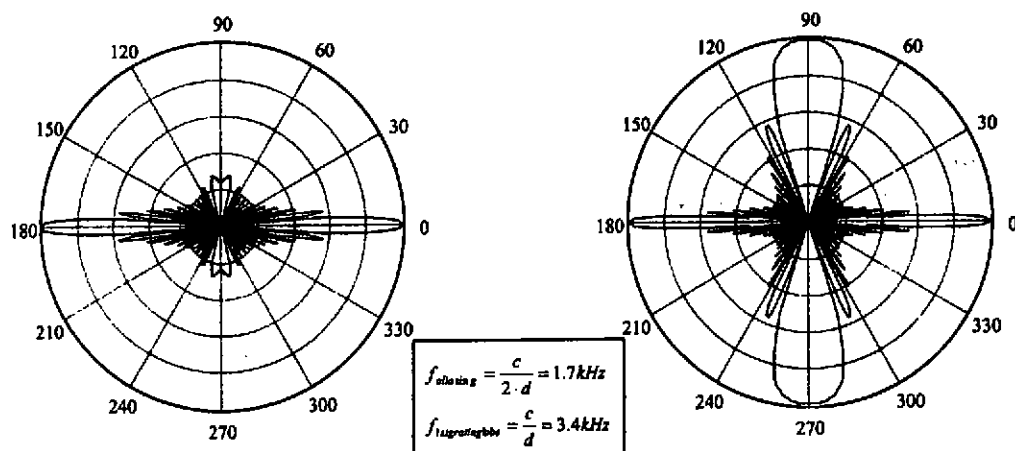


Fig 4 Far field vertical polar showing spatial aliasing, $f = 2.5 \text{ kHz}$ (l) and $f = 3.4 \text{ kHz}$ (r), 6 dB/div.

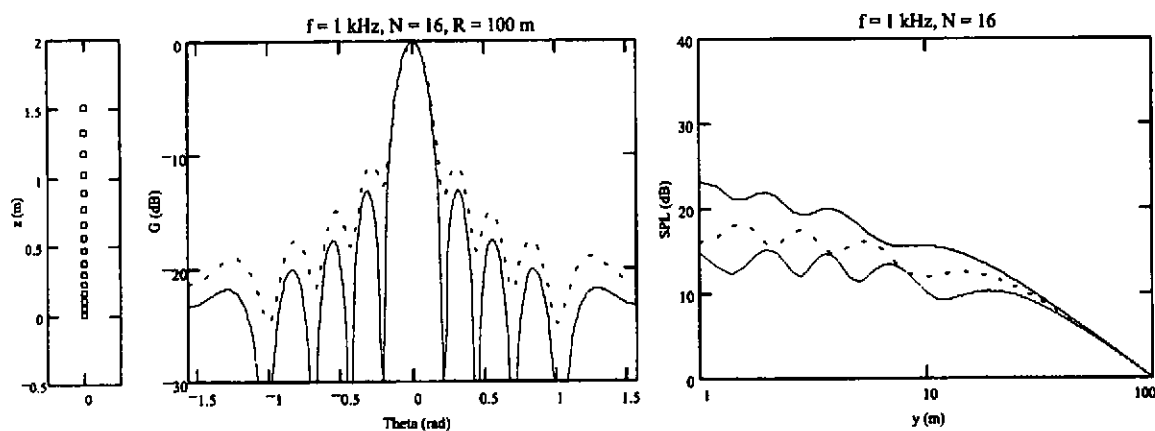


Fig 5 A-symmetrical positioning (l), far field directivity (m) and SPL versus distance (r).

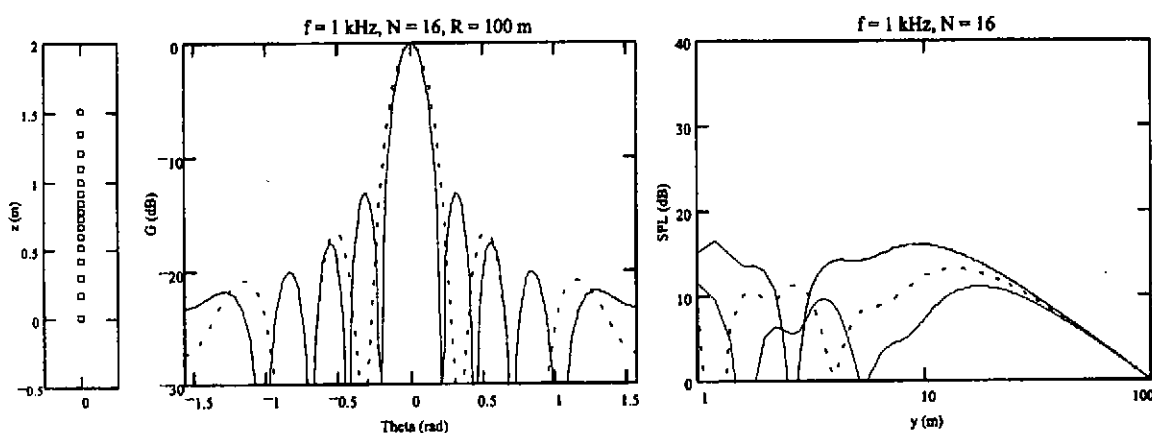


Fig 6 Symmetrical positioning (l), far field directivity (m) and SPL versus distance (r).

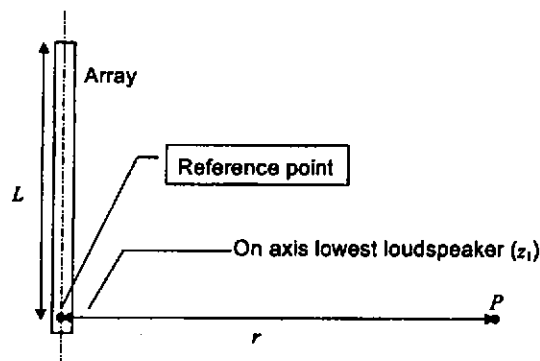


Fig 7 Sketch for far field derivation in case of an a-symmetrical array.

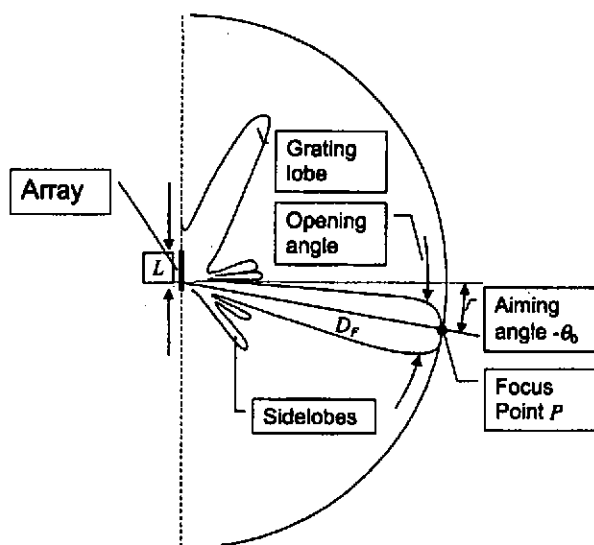


Fig 8 Schematical representation of a far field vertical polar plot ($-90^\circ < \theta < +90^\circ$).

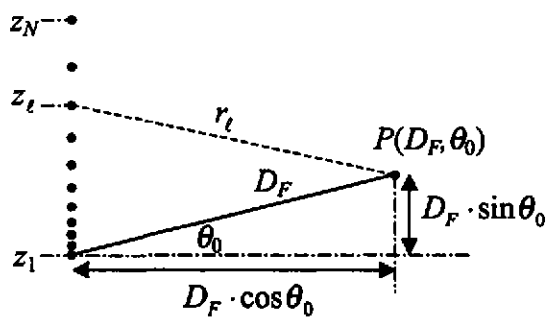


Fig 9 Focus point P and reference z_1 for an a-symmetrical array.

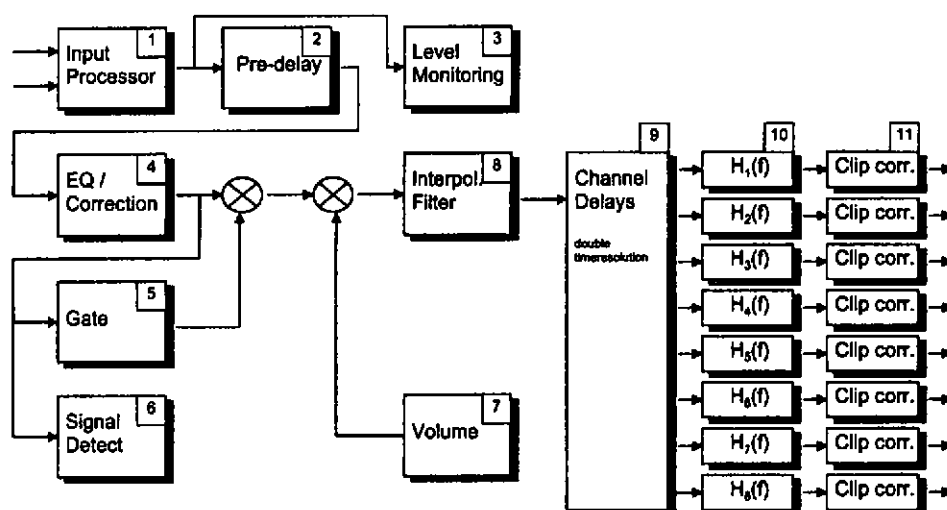


Fig 10 Block diagram of 8 channel 'single lobe' DSP processing.

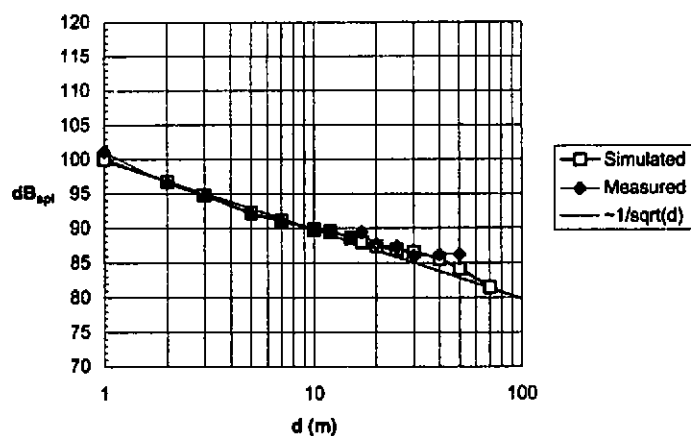


Fig 11 'On axis' 1 kHz octave averaged SPL versus distance for an Intellivox-6c array.

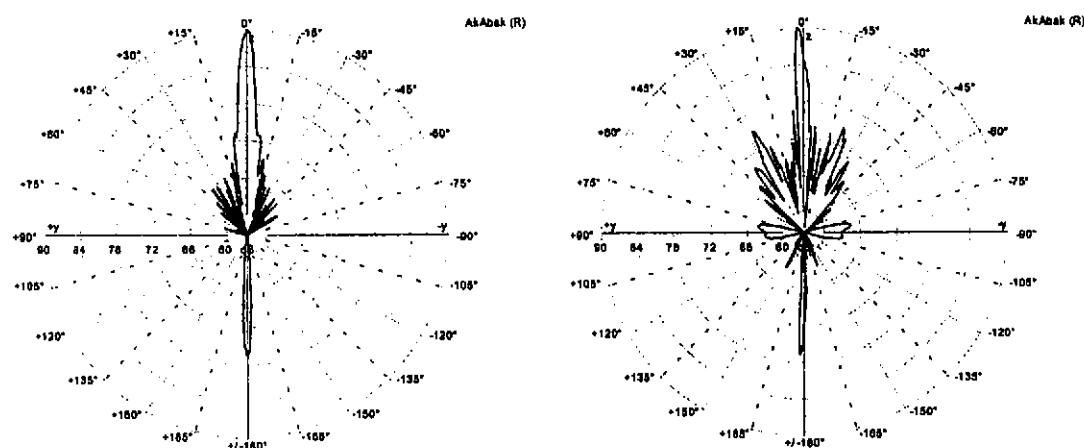


Fig 12 'Processed' (l) and 'un-processed' (r) simulated far field 2 kHz polar of Intellivox-6c.

Proceedings of the Institute of Acoustics

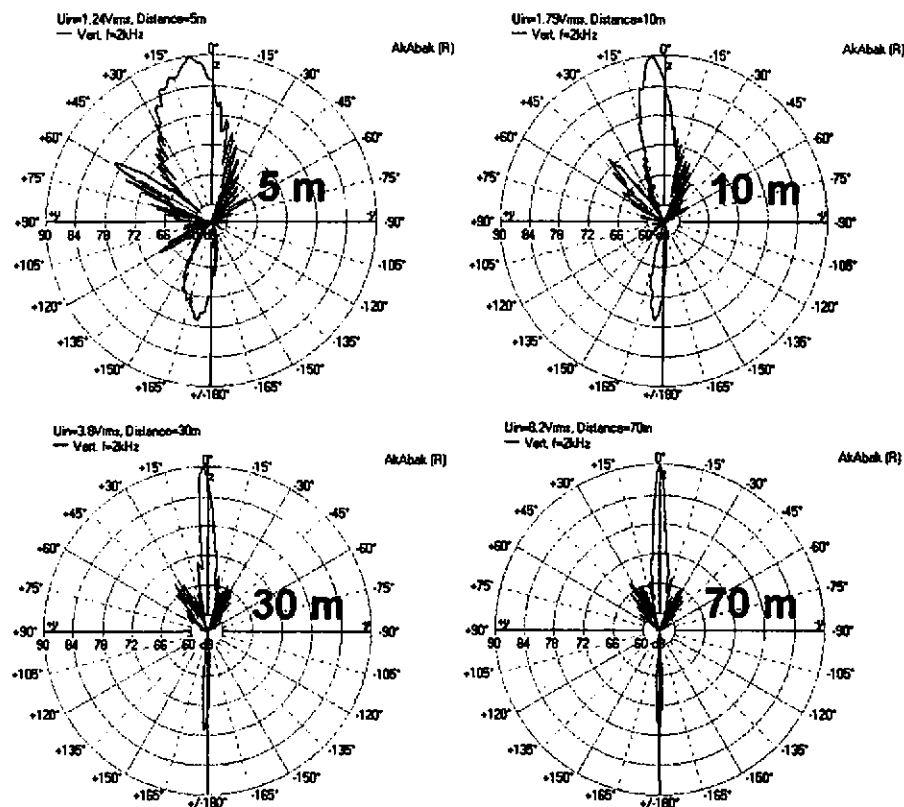


Fig 13 Simulated vertical polar plots of an Intellivox-6c at various distances (2 kHz).

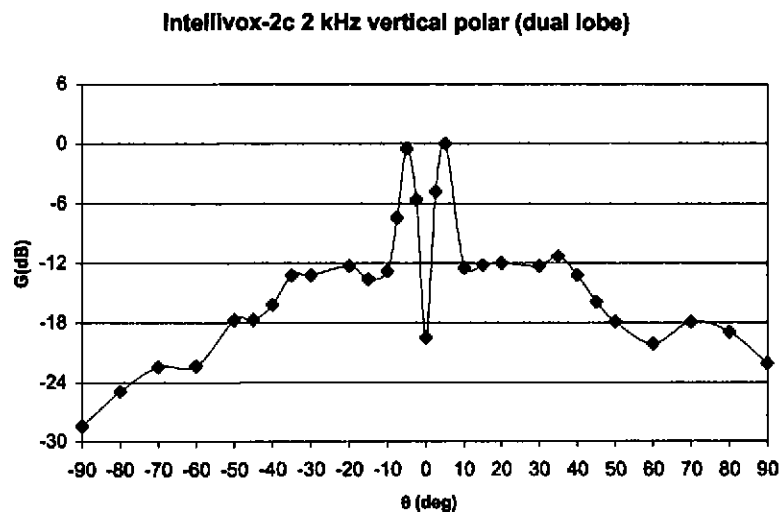


Fig 14 'Dual lobe' example of an 8 channel - 16 element array (measured far field data).

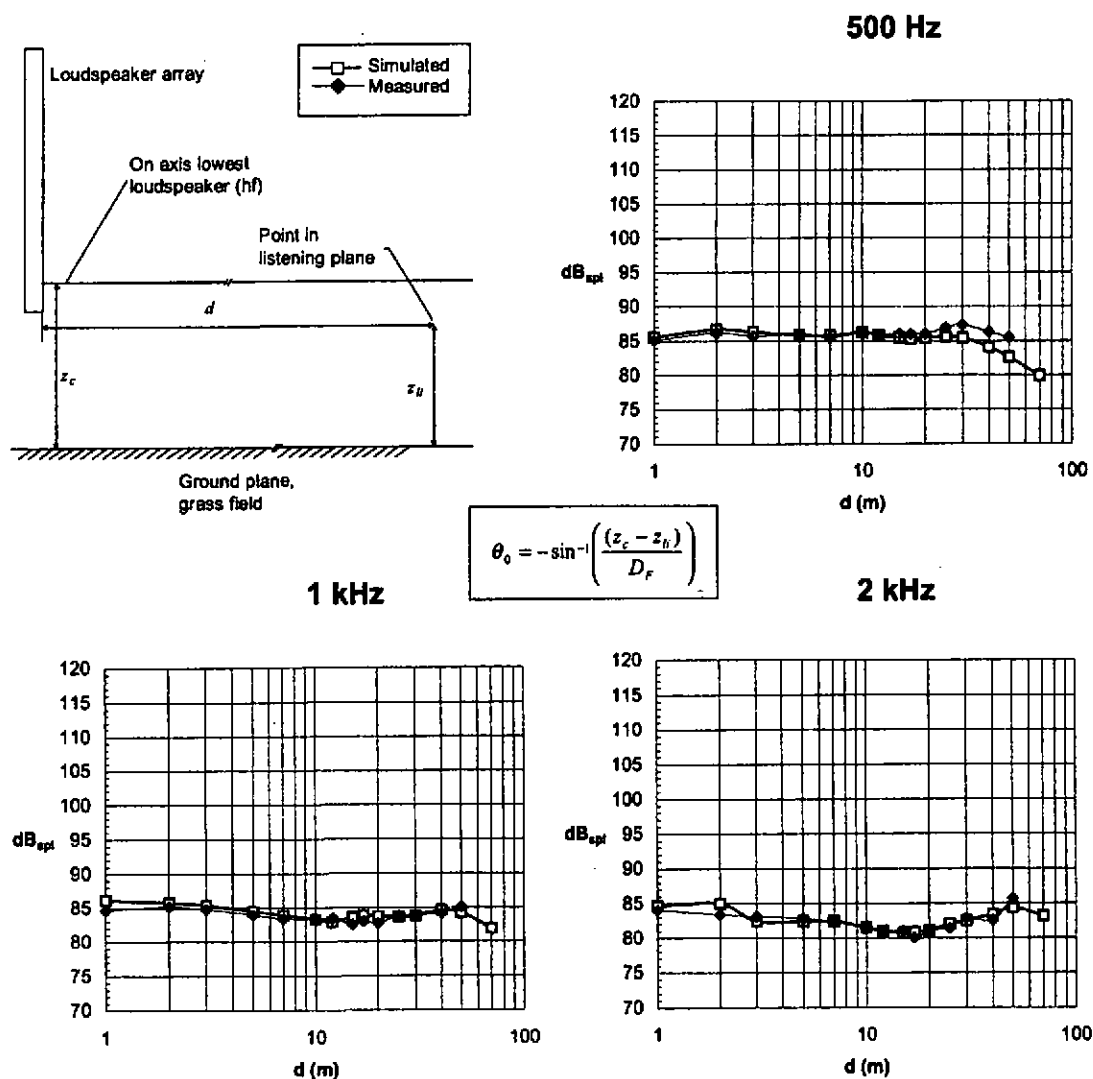


Fig 15 Intellivox-6c SPL versus distance $\theta_0 = -0.9^\circ$ / $op\ angle = 4^\circ$ / $D_F = 70\ m$ / $z_c - z_h = 1.1\ m$.

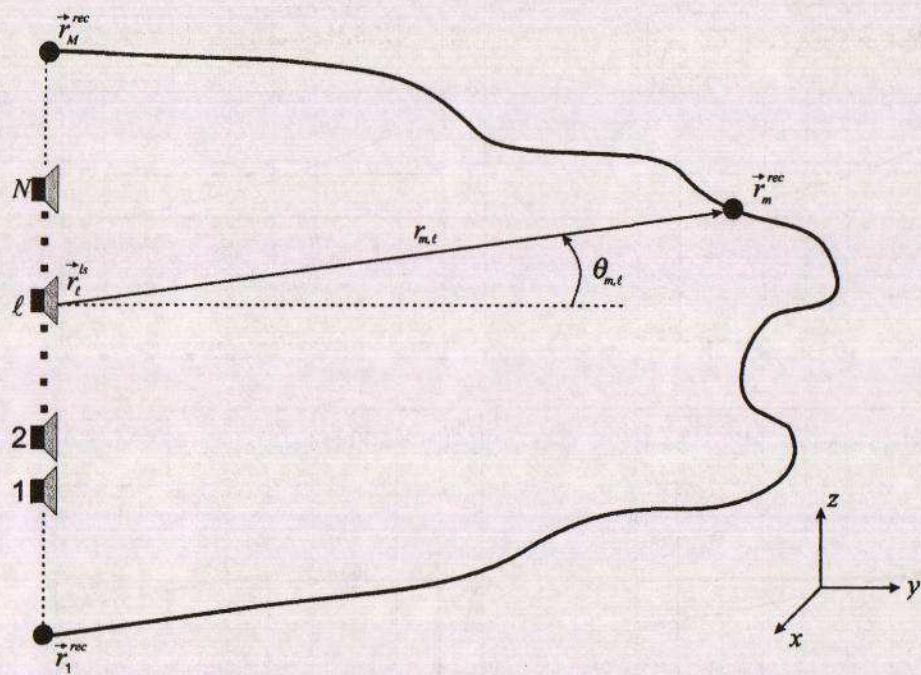


Fig 16 General array configuration.

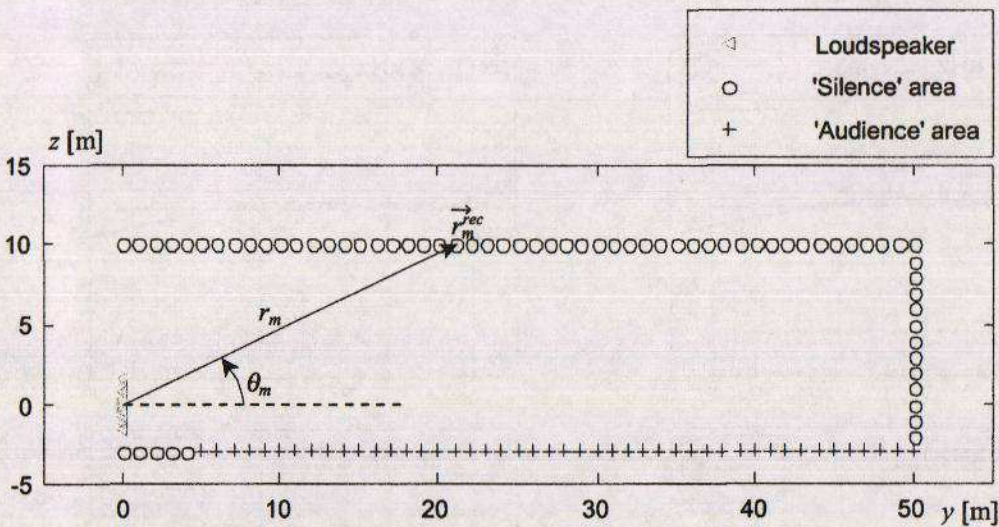


Fig 17 Configuration of complex array optimization method.

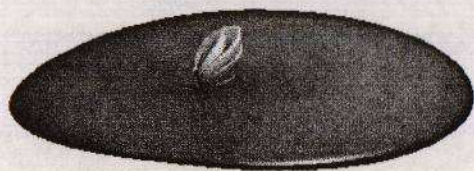


Fig 18 Far field modeled 3-D directivity pattern of FIR optimized array (1 kHz).

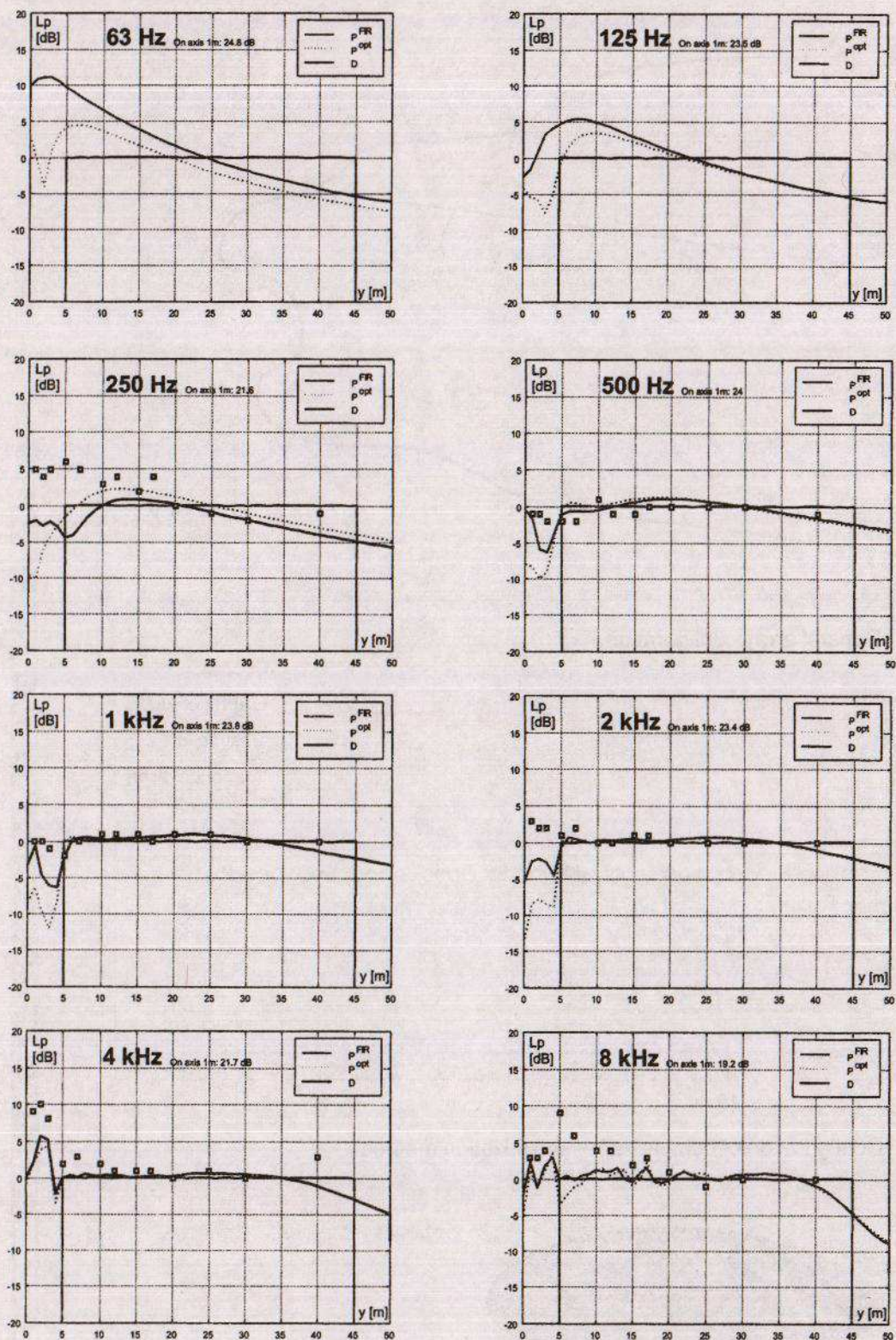


Fig 19 FIR optimized SPL versus distance plots (octave averaged), dots represent measured data.

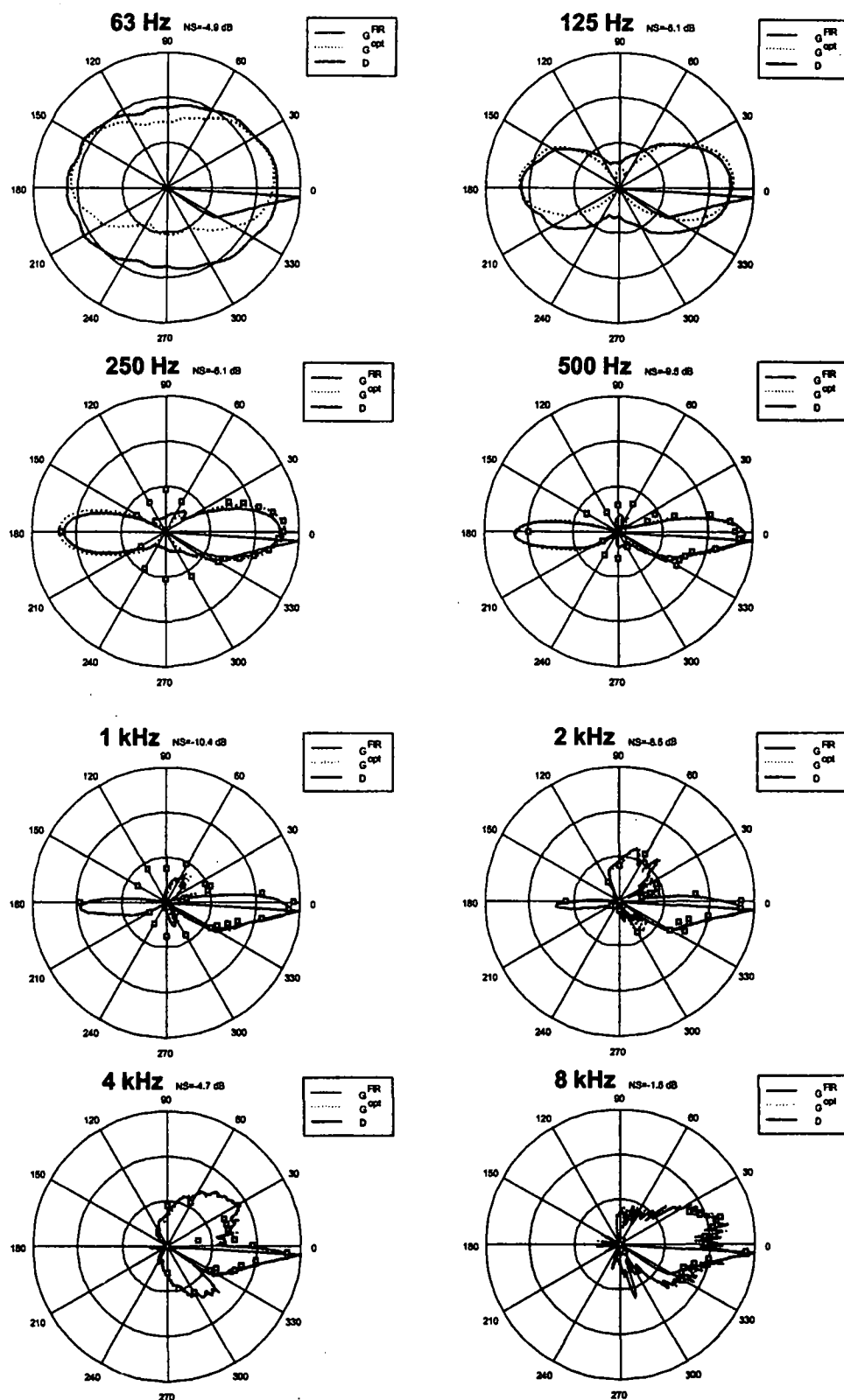


Fig 20 Far field octave averaged vertical polar data of FIR optimized array, scale is 10 dB/div.

